Transactions, SMiRT-25
Charlotte, NC, USA, August 4-9, 2019
Division V

REBAR CORROSION EFFECTS ON ULTIMATE STRENGTH OF UNREINFORCED OR CFRP REINFORCED NUCLEAR COOLING TOWER: THE CASE OF WIND LOADING

Ali Limam[1], Tan Trung Bui[2], Amine Louhi[2], Nicolas Schmitt[3]

[1] IFSTTAR, GERS RRO, Bron, France (ali.limam@insa-lyon.fr)
[2] UDL, INSA de Lyon, France
[3] EDF-DIPNN-CNEPE, Tours, France

ABSTRACT

The French electricity company aims at extending the lifetime of its existing NPP's (nuclear power plants) beyond 40 years, which is its original technical design life-time. The ageing of R.C. structures such as cooling towers should be evaluated and its impact on the bearing capacity calculated. In the case of significant damage, the strengthening must be considered to ensure the sustainability of these towers facing the risk of storms and earthquakes. These loads are certainly the most severe, since they take the structure into the nonlinear domain and can induce or amplify cracking damage.

This work treats the nonlinear behaviour of a French R.C. cooling tower under its own weight and extreme wind pressure or seismic loading. Several simulations are proposed taking into account appearance of concrete cracks and their evolution via an appropriate material concrete law and rebar's yielding. The behaviour of the damaged structure with an advanced level of rebar's section loss is estimated in the pre- and post-cracking regime and compared to the undamaged structure. The evolution of characteristic parameters such as the start of cracking, the yielding of reinforcements and finally the drop of bearing capacity (failure load) are obtained and analysed in different cases of loading and for different geometries.

To restore the integrity and thus increase the lifetime of the structure, a CFRP (Carbon Fiber Reinforced Polymer) retrofit is proposed and studied for different reinforcement configurations. The gain on the bearing capacity and on the different rigidities characterizing the nonlinear load deflection curve are evaluated and discussed. The proposed model and the results found provide useful information to understand the nonlinear behaviour of these structures, and to propose solutions for their retrofit.

INTRODUCTION

The French electricity company analysed the possibility to increase the lifetime of currently cooling towers, first meticulously evaluating ageing RC hyperbolic structures and the impact on the bearing capacity calculated, to determine their lifetime and aid in deciding whether or not to strengthen these structures. In the literature, several studies have been conducted to investigate the ultimate strength of these kind of structures under extreme wind conditions. For example, Mang et al. (1983) presented a comprehensive numerical investigation of the cooling tower at Port Gibson MS (USA) and were the first to assert the representativeness of an incremental calculation concluding that the failure of wind-loaded cooling towers made of reinforced concrete is initiated by rapid propagation of cracks in the tensile zones of such shells followed by activation of the reinforcement until yielding occurs and not by buckling. In

their damage analysis of a cooling tower shell, Harte & Krätzig (2002) noticed that after many years in permanent service, the shells show a considerable number of vertical cracks due to the low amount of reinforcement. The study reported by Baillis et al. (2000), where undamaged and damaged cooling towers were analysed through large parametrical analyses, confirmed the Harte & Kratzig study and demonstrated that in the case of wind load, initial vertical cracks do not significantly reduce the strength. The effect of the initial meridional cracks regularly distributed throughout the shell occurs during the crack plateau, when the shell begins to work in the circumferential direction. All these studies have clarified the failure mechanisms of cooling tower shells and concluded that the reinforcing ratio plays an important role in the ultimate strength of RC cooling tower shells after cracking. Hara (2012) concluded that the ultimate strength is determined by the amount of meridional reinforcement and that fiber reinforced plastic layer strengthening is effective.

In this contribution, the ultimate strength of RC hyperbolic cooling tower is re-investigated. To take into account damage identified on these structures, especially steel corrosion, cooling towers are analysed using the same assumption as Gruber (1996), which consists in reduction of the steel section in the FEM simulations. The several numerical simulations were carried out to study the behaviour in particular the bearing capacity of RC hyperbolic cooling tower in the presence of different levels of corrosion which are approximated by rebar section loss. Then, to restore the integrity of the structure, and therefore to increase its lifetime, the carbon fiber reinforced plastic (CFRP) strengthening technique is explored. A proposed configuration is assessed by quantifying the contribution of CFRP strengthening in terms of stiffness in pre-cracking and post-cracking on a perfect shell or a damaged shell by steel corrosion under extreme wind conditions.

NONLINEAR ANALYSIS

The modelled RC cooling tower is a hyperboloid shell of revolution, reinforced with double-layer rebars grids. The shell is supported on a X-shaped support system and reinforced at the top and the bottom by lintels, which are here modelled by stiffening rings with a high ratio of reinforcement. Tab. 1 shows the dimensions and characteristic thicknesses of the shell. The shell is discretized with shell elements in the circumferential and meridional directions, and the mesh sensitivity study was studied to verify the adopted mesh density.

Table 1: Characteristic dimensions of RC hyperbolic cooling tower

Φ_o [m]	87.56
Φ_u [m]	117.20
Φ_T [m]	83.80
h_s [m]	27.70
h_T [m]	123.20
h [m]	165.50

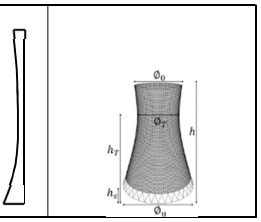

Φ_o: Top diameter Φ_T: Throat diameter e_u: Base thickness e_T: Throat thickness h : Shell height h_s: Supports height h_T: Throat height

Finite element representation

The numerical study was conducted using the finite element program Cast3M, developed at the French Atomic Energy and Alternative Energies Commission (CEA). The elements used for the 3D modelling are triangular three-node elements, with 6 degrees of freedom per node and 3 Gauss points for integration in the plan. These elements called Discrete Kirchhoff Triangle (DKT) are developed by Batoz et al. (1980) and deals with the flexion of thin structures within the framework of Kirchhoff theory. The

thickness of the element representing the concrete is divided into several layers (Fig. 1) working in plane constraints with a concrete model (multi-layered shell element). This approach permits to describe the progression of the damage accurately, in particular crack propagation through the thickness of the shell. The annular footing and the support system are modelled by Timoshenko beam elements (TIMO) with consideration of transversal shear. The boundary conditions reflect a fixed end at the foundation which seems to be a good hypothesis knowing the rigidity of the annular foundation. The shell is reinforced identically on each side with a 3cm concrete cover, the meridian and circumferential reinforcements are represented discretely by eccentric spatial bar elements (BAEX) superimposed on the elements representing the concrete.

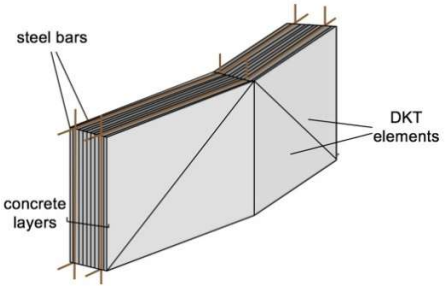

Figure 1. Representation of the element

Reinforced concrete constitutive laws

The concrete model used was developed by Nahas and Millard (1986) within the framework of plasticity theory. In both the tension and compression regimes, this model presents a linear elastic zone followed by a linear softening behaviour (linear drop of stress as strain increases) (see Fig. 2). The cracking of concrete in tension is managed by a Rankine yield function where post-cracking is controlled with a negative softening. Similarly, the crushing of the concrete in compression is represented by a Drucker-Prager-type yield function with isotropic negative softening. ε_u is the ultimate compressive strain. To limit strain localization and mesh sensitivity, a Hillerborg approach is used to ensure that cracking energy G_f is an "objective" material parameter, and ε_{tu} the ultimate tensile strain varies depending on the size of the finite element.

For the meridian and circumferential reinforcements, the behaviour is assumed to be elasto-plastic with positive hardening. The steel rebar behaviour is illustrated by the graph in Fig. 3. Tab. 2 shows the mechanical properties of each material.

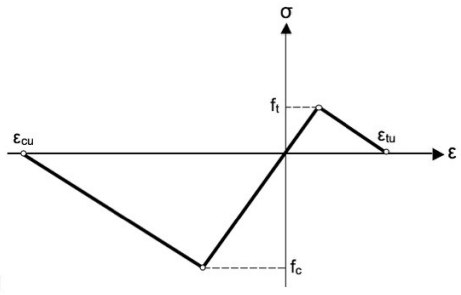

Figure 2. Stress-strain relationship of Nahas-Millard concrete model

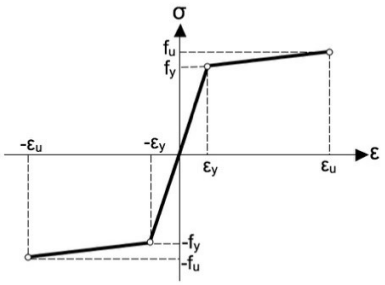

Figure 3. Stress-strain relationship of steel

Table 2: Materials properties

	Shell concrete	Steel bars
Elastic modulus E_c [GPa]	33.378	210
Poisson ratio ν	0.2	0.3
Uniaxial compressive strength f_c [MPa]	28.7	-
Uniaxial tensile strength f_t [MPa]	2.3	-
Initial yield stress f_y [MPa]	-	400
Ultimate stress f_u [MPa]	-	444
Ultimate strain ε_u	-	11%

Applied load

To study the nonlinear response of the cooling tower when subjected to dead load and wind pressure, a numerical analysis taking into account the nonlinear behaviour of the constitutive materials was conducted. Once the dead load is applied, the pressure associated with the wind effect is incremented via a multiplying factor load λ, while the dead load is kept constant. Wind load is simulated by a pressure decomposed into Fourier series on the circumference and varies depending on height, as recommended by the Cahier des Règles Techniques [CRT], which is based on the NV 65 rules (2009). These rules incorporate all the modifications, including wind and snow maps to ensure consistency with the [Eurocode 1]. The dynamic pressure is defined by:

$$P_v^{ref} = (q_{10} \,.\, C(z).\, g(\theta).\, C_r \,.\, C_m \,.\, C_d \,.\, \beta) + S \qquad (1)$$

q_{10} is the basic dynamic pressure exerted at a height z = 10 m above the ground and expressed in daN/m² given by:

$$q_{10} = \frac{V^2}{16.3} \qquad (2)$$

V is the extreme wind velocity in m/s defined by the table of wind speeds corresponding to dynamic pressures for different zones, according to the NV 65 rules. The wind speed here taken into account is 41.40 m/s, in ad equation with the zone where the cooling tower was built. The coefficient C(z) takes into account the effect of the height above ground. The resulting distribution pressure is variable over the structure, including an angular distribution function which corresponds to a Fourier series decomposition of ten terms given by the function:

$$g(\theta) = \sum_{k=0}^{10} a_k \; cos\, k\theta \qquad (3)$$

Reduction factors C_r, C_d and C_m are introduced in NV 65 rules to take into account the effect of roughness, the dimension effect and the interference effect, respectively. (Orlando, 2001) studied the wind-induced interference effects on two adjacent cooling towers and obtained a minimum distance to avoid interference quite near to the minimum distance of the French Standards. The CRT recommends not taking into account any reduction. However, the required dynamic effect coefficient is $\beta = 1.2$. The internal pressure induced by the wind is assumed to be uniform $S = -0.4\,q$. Where q is the dynamic pressure at the top of the tower.

NUMERICAL RESULTS AND DISCUSSION

The overall response of the tower is shown in Fig. 4. Our observations agree with Jia's (2013) behavior analysis of the Port Gibson cooling tower. The most stressed point is often found in the thinnest part of the shell (the throat). The calculation shows that cracks begin to appear in the vicinity of this point at the load factors mentioned in Tab. 3. Fig. 5 shows the radial displacement of the tower. By increasing the load, the stiffness of the structure gradually decreases. This decrease is due to crack initiation and propagation; however, the structure continues to sustain the load by the activation of the load-carrying capacity of the reinforcement, which inhibits cracks opening. Finally, the collapse of the tower is not due to the achievement of the steel's ultimate strain but by the combination of significant damage (cracks spread along the meridional and circumferential directions) and severe propagation of cracks in thickness layers, coupled to the steel yielding. Applied subsequent load even very low increments may not be sustained and redistributed on the shell. These results are also compared to the studies of Krätzig et al. (1998) and Witasse et al. (2002) (Fig. 4). The difference appearing at the cracking loads and failure loads is related to the slenderness and the shape of each cooling tower.

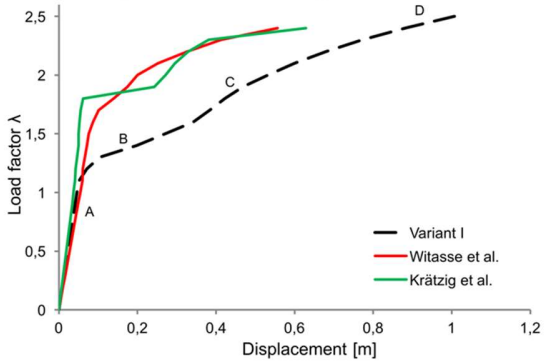

Figure 4. Comparison of load-displacement curves

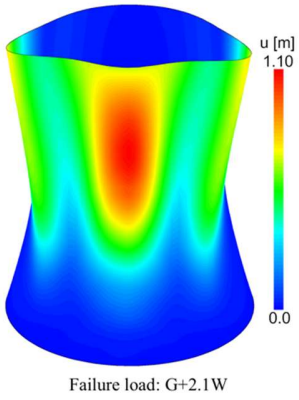

Figure 5. Radial displacement isovalues

Table 3: Crack and failure load amplitudes (baseline simulation)

Height of the most deformed point [m]	139.66
λ multiplying wind factor of crack load	1.4
λ multiplying wind factor of steel yielding	1.6
λ multiplying wind factor of failure load	2.1
Steel strain at failure load	1.09%

Influence of rebar corrosion

In fact, the corrosion process involves mainly two major effects. Firstly, an expansion of the rust products occurs, leading to the cracking and eventually the spalling of the cover concrete and generating variations of steel concrete bond strength, and secondly, the brittleness of the steel increases although its cross-section decreases uniformly or by pitting depending on type of aggressive agent Richard et al. (2010); Idrissi & Lima (2003). In the case reported herein, only the reduction of the steel cross-section is taken into account. Two cases of rebar cross-section diminution (20% and 40%) are here studied. The two configurations are extremely pessimistic and not representative of the actual observations which confirm, only the initiation of corrosion in some points of the structure. More than that, the monitoring of the different cooling towers, permits to repair the corroded steel reinforcement, by cleaning and application of inhibitors of corrosion.

The results (Fig. 6) show that the level of the bearing capacity is significantly reduced by 19.05%, assuming a degree of corrosion of 40%. The cracking load factor λ decreases slightly by increasing the corrosion rate (see Tab. 4). The length of the cracking plateau increases as the corrosion rate increases, confirming that it depends on the percentage of steel. In addition to the clear reduction in the structure's safety, a dramatic decrease in sustainability is expected due to the increase of the number of cracks in the tension part.

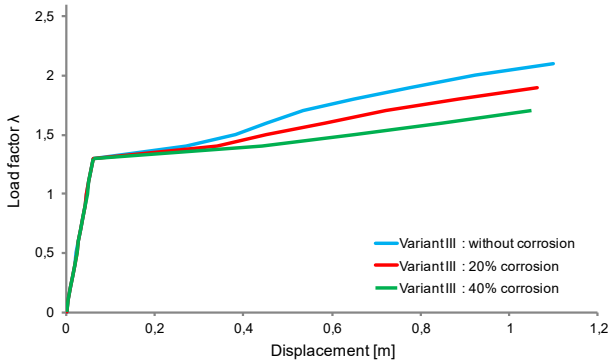

Figure 6. Load-displacement curves of the most deformed point with and without corrosion

Table 4: Crack and failure load amplitudes (corrosion simulations)

	20% corrosion	40% corrosion
Height of the most deformed point [m]	141.16	144.16
λ multiplying wind factor of crack load	1.4	1.3
λ multiplying wind factor of steel yielding	1.5	1.4
λ multiplying wind factor of failure load	1.9	1.7
Steel strain at failure load	1.09%	1.10%

Contribution of the CFRP

To gauge the effect of retrofit using Carbon Fiber Reinforced Polymers (CRFP), a new simulation is conducted, keeping the same material and dimension characteristics of the structure, and integrating CFRP belt layers (all around the circumference, starting from 40.47 m above the base to the top of the shell and without strengthening the crown. Forty one (41) rings are considered. The height Z=40.47 m represents the beginning of displacement accentuation found in the above-reported calculations. CFRP strengthening was modelled by adding eccentric layers to the DKT elements representing the thickness of the composite reinforcement. The associated behavior is elastic orthotropic, the material properties of the CFRP strips are given in Tab. 5. Fig. 7 shows a view of the built model.

Table 5: CFRP material properties

Elastic modulus $E1_c$ [GPa]	105
Elastic modulus $E2_c$ [GPa]	45
Thickness [mm]	0.48

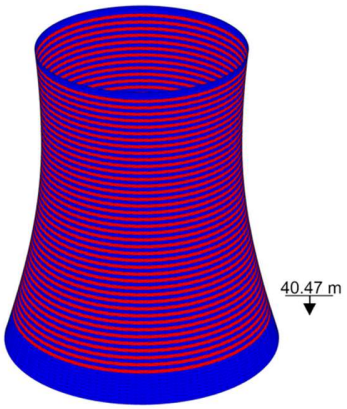

Figure 7. View of the reinforced concrete shell

CFRP strengthening allows a meaningful gain of 16% of the structure's bearing capacity compared to the results of the non-reinforced structure, increasing from G+2.1W to G+2.5W (see Fig. 8). The cracking load and stiffness in the elastic phase remains nearly identical. The results show a significant reduction in displacements in both configurations reaching 50% at the throat which is very beneficial for the integrity of the structure. As shown in Tab. 6, the CFRP strengthening delays the yielding of the steels. However, the behavior of the cracked concrete became more fragile.

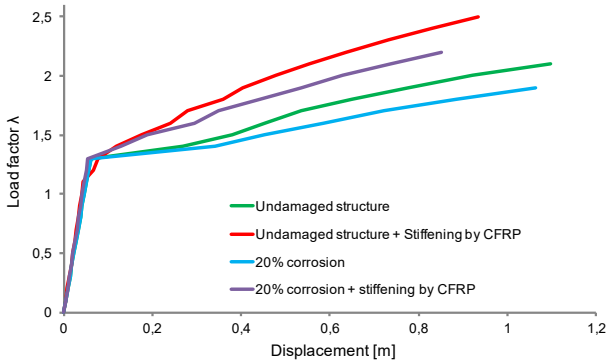

Figure 8. Behaviour of the reinforced and non-reinforced structure – point at 139.66 m of attitude

Table 6: Crack and failure load amplitudes (Corrosion + CFRP simulations)

	undamaged structure + CFRP	20% corrosion + CFRP
Height of the most deformed point [m]	129.17	124.67
λ multiplying wind factor of crack load	1.4	1.4
λ multiplying wind factor of steel yielding	1.8	1.5
λ multiplying wind factor of failure load	2.5	2.2
Steel strain at failure load	1.06%	1.12%

Finally, to gauge the benefits of CFRP on a damaged structure, a 20% corroded tower is considered, which is, as mentioned before, a drastic rebar section diminution. The reinforcement detailed above is reused, with the results detailed in Fig. 8 and Tab. 6. CFRP stiffening restores the original bearing capacity (undamaged structure) and even improves the latter by 5%: the failure load increases from G+2.1W to G+2.2W. The initial stiffness increases slightly.

CONCLUSION

The problems associated with the ageing of a RC cooling tower shell are here taken into account through simple assumptions of degradation scenario, as here with rebar section loss, this methodology can provide an estimation of the actual bearing capacity.

The loss of rebar's section induced by corrosion, conducts to a drop of the load associated to crack initiation. This means that classical gusts higher than or equal to 120 km/h, which generally occur every 5 years, are going to increment crack appearance and propagation, therefore enhancing the risk of premature ageing. Corrosion degree strongly affects the ultimate state: 40% of corrosion induces approximatively 19% loss of the structure's bearing capacity. This estimation needs to be revisited taking into account the loss of adherence between the steel and the concrete, which is assumed to be perfect in our calculations. Also, corrosion conducts generally to a strain hardening reserve diminution, this have to be studied in a future work. But we underline again, that the corrosion currently observed on cooling towers is very far from the levels here studied.

Finally, CFRP reinforcement is highly beneficial in terms of bearing capacity. The latter increased by 16% compared to the non-damaged non-reinforced (only rebar and no CFRP layers) structure. There is also a significant decrease in displacements, which can reach 50% at the throat. The

CFRP reinforcement also makes it possible to exceed 5% bearing capacity in a structure that has lost 20% of the rebar reinforcement section. Adding this process is advantageous to extend the life of damaged structures provided that noncontinuous CFRP reinforcement is considered (discrete strips) to avoid changing the water equilibrium developed after years of service.

REFERENCES

Baillis, C., Jullien, J.F., Limam, A. (2000). "An enriched 2D modelling of cooling towers. Effects of real damage on the stability under self-weight and on the strength under wind pressure", *Engineering Structures*, 22, 831 – 846.

Batoz, J.L., Bath,e K.J., Ho, L.W. (1980). "A Study of Three-Node Triangular Plate Bending Elements", *International Journal for Numerical Methods in Engineering*, 15, 1771 – 1812.

Cahier des Règles Techniques (CRT) (1992). *Ouvrages en béton des réfrigérants atmosphériques humides à contre-courants et tirages naturels : Clauses générales*, Version division, Document EDF, Référence 56.C.005.01, 45p. (In French).

Gruber, K.P. (1996). "A new design concept to increase the safety and durability of cooling tower shells", *Proceedings of the 4th International Symposium on Cooling Towers*, 305 – 312.

Hara, T. (2012). "Numerical Evaluation of Repaired Cooling Tower Shell after Damaging", *Proceedings of the 6th International Symposium on Cooling Towers*, 239 – 345.

Harte, R., Krätzig, W.B. (2002). "Large-scale cooling towers as part of an efficient and cleaner energy generating technology", *Thin-Walled Structures*, 40, 651 – 664.

Idrissi, H., Limam, A. (2003). "Study and characterization by acoustic emission and electrochemical measurements of concrete deterioration caused by reinforcement steel corrosion". *NDT & E International*, 36, 563 – 569.

Jia, X., (2013). "Revisiting the failure mode of a RC hyperbolic cooling tower, considering changes of material and geometric properties", *Engineering Structures*, 47, 148 – 154.

Krätzig, W.B., Konke, C., Mancevski, D., Gruber, K.P. (1998). "Design for durability of natural draught cooling towers by life-cycle simulations", *Engineering Structures*, 20, 899 – 908.

Louhi, A., Limam A., Merabet O., Rourre T., « Rebar Section Loss and Carbon Fiber Reinforced Plastic Reinforcement Effects on Nonlinear Behavior and Ultimate Load of Cooling Towers". *Engineering Structures,* 136 (2017) 481–493.

Mang, H.A., Floegl, H., Trappel, F., Walter, H. (1983). "Wind-loaded reinforced-concrete cooling towers: buckling or ultimate load?", *Engineering Structures*, 5, 163 – 180.

Nahas, G. (1986). *Calcul à la ruine des structures en béton armé*. PhD Thesis: University of Paris VI, 210p. (In French).

Orlando, M. (2001). "Wind-induced interference effects on two adjacent cooling towers". *Engineering Structures*, 23, 979 – 992.

Règles NV 65 (2009. *Règles définissant les effets de la neige et du vent sur les constructions et annexes*, CSTB DTU P 06-002, 220p. (In French).

Richard, B., Ragueneau, F., Cremona, C., Adelaide, L., Tailhan, J.L. (2010). A" three-dimensional steel/concrete interface model including corrosion effects", *Engineering fracture Mechanics*, 77, 951 – 973.

Witasse, R., Georgin, J.F., Reynouard, J.M. (2002). "Nuclear cooling tower submitted to shrinkage; behaviour under weight and wind", *Nuclear Engineering and Design*, 217, 699 – 716.

Zhao, L., Ge, Y.J. (2010). "Wind loading characteristics of super-large cooling towers", *Wind and Structures*, 13(4), 257 – 274.